On the Potential Vorticity Structure of Weakly Ventilated Isopycnals: A Theory of Subtropical Mode Water Maintenance

WILLIAM K. DEWAR*

Curriculum in Marine Sciences, University of North Carolina, Chapel Hill, NC 27514

(Manuscript received 19 September 1985, in final form 8 January 1986)

ABSTRACT

A two-layer model of the general circulation including wind and thermal forcing is discussed. The flow in each layer is geostrophic, hydrostatic and obeys linear potential vorticity constraints. The equations are developed in spherical coordinates and reduce to a surprisingly simple, coupled, nonlinear set. Analytic solutions of this system are obtained in the quasi-geostrophic limit. The novel feature in this model is a weakly ventilated and weakly dissipative lower layer.

The quasi-geostrophic model predicts homogenized potential vorticity in regions of the lower layer which are not directly ventilated. These are also regions of locally minimum value in potential vorticity. The net balance determining the potential vorticity structure is between the diabatic forcing of the lower layer and eddy-driven mixing. As such, the structure of the solution depends on the sign of the eddy diffusion of potential vorticity (positive) and the sign of the diabatic potential vorticity source (negative). It is therefore argued that these features are not dependent on quasi-geostrophy.

A comparison of model results with data is encouraging. The 26.5 sigma-theta isopycnal is argued to be a density surface to which this theory applies. The potential vorticity structure on this surface obtains a bowl-like shape and agrees well with the model. The subtropical mode water of the North Atlantic (18°C water) is centered on this isopycnal and is identified in the model as the homogenized local potential vorticity minimum. The stability of 18°C water characteristics, documented elsewhere, is explained in terms of a gyre-scale response to variability.

1. Introduction

The linear potential vorticity balance:

$$\beta v = f w_z, \tag{1}$$

where f is the Coriolis parameter, β its north–south gradient, v north–south velocity, w vertical velocity and subscripts denote differentiation, and its vertical integral:

$$\beta \int_{-H}^{0} v dz = f w_e \tag{2}$$

(w_e is the Ekman pumping at the mixed layer base) the "Sverdrup relation," are at the center of general ocean circulation theory. The studies of Warren (1970) and Leetma, Niiler and Stommel (1977) suggest strongly that the Sverdrup relation accurately describes the depth integrated, wind-driven, large-scale flow. In view of this success, a number of investigators have tried to augment Eq. (2) with theories which fit within the Sverdrup relation and resolve issues it does not address. One area of recent interest is the vertical structure of the general circulation; note that Eq. (2) makes no attempt to compute this structure.

The recent lines of thought about the vertical structure of the circulation have proceeded in two distinct ways. Rhines and Young (1982a,b) and Young and Rhines (1982) have considered quasi-geostrophic layered circulation models. The upper layer in these models is directly driven by the wind and the lower layers are accelerated by eddy form drag. The gyres respond to the winds by forming regions which are isolated from the eastern boundary. Eddy form-drag, although weak in magnitude, maintains a mean flow in these areas, thus trapping some of the Sverdrup transport in the lower layers. The characteristics of the Rhines and Young solutions include the homogenization of potential vorticity within closed geostrophic contours and the northward migration of gyre center with depth. Both features have now been documented in the North Pacific (Keffer, 1985) and the North Atlantic (McDowell et al., 1982).

The second approach to determining the vertical structure of the general circulation is based on thermocline ventilation. This theory, proposed by Luyten et al. (1983), predicts the thermocline structure by tracing back on characteristics to locations where the fluid has been altered by atmospheric interaction. Fluid columns after subduction conserve potential vorticity

* Present Address: Dept. of Oceanography and Supercomputer Computations Research Institute, Florida State University, Tallahassee, FL, 32306.

and therefore move in curved paths to the southwest. The boundary between active and motionless fluid in a subducted layer is determined by the characteristic, or line of constant potential vorticity, which strikes either the western or northern boundary. The net transport in ventilated models is determined by the Sverdrup relation (Eq. 2). The manner in which this transport is partitioned between ventilated and subducted layers is also fixed by the positioning of the constant potential vorticity characteristics. Pedlosky and Young (1983) in a companion paper have described how unventilated layers are set into motion by vertical eddy stresses. Ventilated thermocline theories predict the northward migration of gyre center with depth, as does the Rhines and Young theory. Luyten et al. also argue that their solutions possess weak potential vorticity structure across the basin, and are therefore consistent with the field observations of uniform potential vorticity.

There is a major difference in the philosophy of the above two approaches. Rhines and Young (1982a,b) stress the importance of weak, nonconservative eddy mixing, while the structure predicted by Luyten et al. (1983) depends upon exact conservation of potential vorticity.

Both theories are enlightening but contain certain incompletely resolved issues. It is likely, for example, that eddies play some role in ventilated layers. This is suggested by the solutions in Luyten et al. and the observations of McDowell et al. (1982). In both cases, the gradient of potential vorticity is observed to reverse with depth in the westward interior return flow. Such a region should be baroclinically unstable and a source region for eddies. One would expect these eddies to have an effect on the mean flow. How eddies can be included in ventilated thermocline theories and what their effects might be have not been addressed. Second, ventilated theories do not resolve the general circulation structure in regions which are not directly ventilated (i.e., not connected to outcropping regions via characteristics). Luyten et al. (1983) and Pedlosky and Young (1983) have used uniform potential vorticity in these unresolved areas, but stress that this is an ad-hoc assumption. Rhines (1984) argues on the basis of the "recirculation index" that directly ventilated flow is only ~20% of the total Sverdrup transport and thus that resolution of the flow in unventilated regions is of primary importance. With respect to the quasi-geostrophic Rhines and Young theories, their analysis elegantly demonstrates the importance of eddies, but is restricted by the lack of ventilation and outcropping layers.

The present paper presents a model of the ventilated thermocline with eddy mixing and addresses in a limited way several of the above points. Scaling arguments are used to reduce the planetary geostrophic equations to a hybrid model containing elements of ventilation and quasi-geostrophic theory. The strict application of the results in this paper are to layers which are "weakly" ventilated and "weakly" dissipative (weakly to be clarified shortly). A comparison of predictions with data suggests however that the model transcends the strict parameter ranges of its validity and describes layers with relatively strong ventilation.

Regions which are not directly ventilated experience the effects of ventilation because of eddy mixing. The structure within these regions can be calculated, as opposed to specified, within the model. The homogenization of potential vorticity emerges within the unventilated regions; a somewhat surprising result as the boundary conditions at the outermost unventilated streamline are different than those which were applied in Rhines and Young (1982a). The potential vorticity on directly ventilated characteristics is also affected by eddy mixing. It is shown that the circulation structure is determined by a balance between buoyancy forcing and eddy mixing. The ramifications for the existence and stability of subtropical mode waters (e.g., 18°C water in the North Atlantic) are discussed.

2. Model development

Consider the two layer model in Fig. 1. The Coriolis parameter, f, varies with latitude, the bottom is assumed to be flat and Ekman pumping, w_e, is imposed at the upper surface. It will be convenient later to express the position of the interface at $z = -h$ as

$$h = -H_0 + \eta$$

where H_0 is half the total fluid depth and η is the deviation of the interface from H_0. This notation is similar to that used in quasi-geostrophic theory. Scaling will be adopted later which will restrict the present model to the quasi-geostrophic parameter range; however, it is important to note that no restrictions have as yet been placed on the size of η. The dynamical

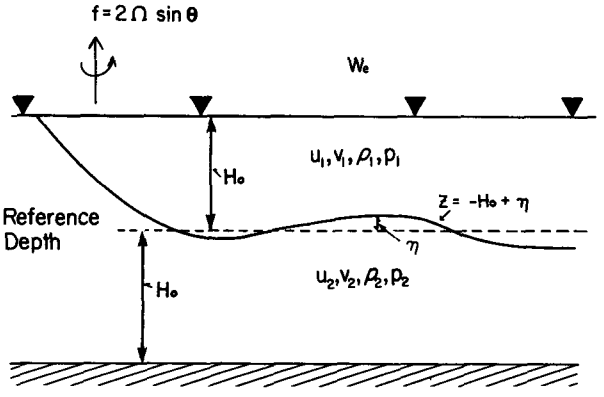

FIG. 1. Model System. The upper layer is subject to a downward Ekman pumping. The lower layer experiences ventilation through diabatic forcing. Both layers are constant density and the ocean bottom is assumed flat.

equations within each layer are the geostrophic equations:

$$fv_i = (a\cos\lambda)^{-1}\tilde{p}_{i\varphi} \tag{3}$$

$$fu_i = -a^{-1}\tilde{p}_{i\lambda} \tag{4}$$

the hydrostatic equation:

$$\tilde{p}_{iz} = -\rho_i g \tag{5}$$

and mass conservation:

$$(a\cos\lambda)^{-1}[u_i]_\varphi + (a\cos\lambda)^{-1}[(\cos\lambda)v_i]_\lambda + (w_i)_z = 0. \tag{6}$$

Here λ is latitude, φ longitude, z height, $u(v)$ east (north) velocity, $\tilde{p}$ 'reduced' pressure, ρ density, g gravity and f the Coriolis parameter. The subscript i denotes the layer and the classical thin-shell assumption has been used in Eqs. (3), (4) and (6) to replace the radial coordinate r with the mean earth radius a.

Substituting in Eq. (6) for u_i and v_i with the geostrophic equations yields Eq. (1), the linear potential vorticity constraint. Equations (3)–(5) insure Taylor-Proudman flow in each layer, and Eq. (5) may be rewritten as

$$p_2 - p_1 = g'\eta, \tag{7}$$

where

$$\left.\begin{aligned} p_i &= \tilde{p}_i + g\rho_i z + g\rho_i H_0 \\ g' &= g(\rho_2 - \rho_1)/\rho_0 \end{aligned}\right\}.$$

Integrating Eq. (1) vertically over each layer yields

$$\beta v_1 h = f[w_e - w_1(x, y, -h)] \tag{8a}$$

$$\beta v_2 \hbar = f w_2(x, y, -h) \tag{8b}$$

where $w_i(x, y, -h)$ denotes the vertical velocity at the interface; h and $\hbar$ are the upper and lower layer thicknesses, respectively, and it has been assumed that w vanishes at the bottom of the ocean.

a. The boundary condition at the interface

Because of the presence of atmospherically-driven heat fluxes in the upper ocean, the calculation of $w_i(x, y, -h)$ in Eqs. (8) must be made by considering the heat budget of the upper layer, which is

$$h_t + (a\cos\lambda)^{-1}u_1 h_\varphi + a^{-1}v_1 h_\lambda + w_1 = D - F_s/(\Delta T) = D + S \tag{9}$$

where ΔT is the difference in the layer temperatures, F_s is the heat flux from the ocean to the atmosphere occurring at the surface and D denotes the eddy-driven lateral thickness fluxes occurring at the interface. The formal derivation of Eq. (9) proceeds by considering the heat equation for a continuously stratified fluid in the limit of a rapidly varying temperature profile and is given in appendix A. Solving Eq. (9) for $w_1(x, y, -h)$ yields

$$w_1(x, y, -h) = -h_t - (a\cos\lambda)^{-1}u_1 h_\varphi - a^{-1}v_1 h_\lambda + S + D. \tag{10}$$

Thus $w_1(x, y, -h)$ is composed of three parts: one part due to the motion of the isopycnal, another due to atmospherically driven heat fluxes and the third due to lateral buoyancy fluxes. The latter has been discussed by Rhines and Holland (1979) and is the mechanism responsible for the lateral potential vorticity diffusion parameterization employed by Rhines and Young (1982a). The second quantity, S, contains diabatic effects and expresses the cross-isopycnal flow caused by the heat fluxes. If the fluid is being cooled by air–sea exchange, i.e., if $F_s > 0$, S is negative. This corresponds to a tendency for the upper layer to become thinner ($h_t < 0$), or equivalently for the system to locally convert warm water to cold water to accomodate the heat loss. A negative value of F_s implies a gain of heat by the ocean and a corresponding tendency for the upper layer to thicken.

Finally:

$$w_2(x, y, -h) = w_1(x, y, -h),$$

as required by continuity [Eq. (6)] and geostrophy [Eqs. (3) and (4)].

If Eqs. (8) are added together, a version of the linear potential vorticity balance is obtained:

$$\beta H_0 f^{-1}\theta_x + [\beta/(2g'f)](\psi^2)_x = f w_e \tag{11}$$

where

$$\left.\begin{aligned} \theta &= p_1 + p_2 \\ \psi &= p_2 - p_1 \end{aligned}\right\}$$

and the coordinate system has been formally transformed from the (λ, φ) system to a "warped" Cartesian system whose independent coordinates are defined by

$$\left.\begin{aligned} x &= a\cos(\lambda)(\varphi - \varphi_0) \\ y &= a(\lambda - \lambda_0) \end{aligned}\right\}.$$

Here φ_0 is a reference longitude and λ_0 is a reference latitude. Integrating Eq. (11) yields

$$[\beta H_0/f]\theta + [\beta/(2g'f)]\psi^2 = \phi \tag{12}$$

where

$$\phi = -\int_x^{x_e} f w_e dx$$

is a prescribed function and the boundary conditions:

$$p_1 = p_2 = 0$$

on the eastern ocean boundary, $x = x_e$, have been applied. Equation (12) is a form of the Sverdrup balance, and is an analog of an equation which appeared in Luyten et al. (1983) and Pedlosky and Young (1983).

Upon subtracting the layer equations [Eqs. (8)] we obtain

$$2\psi_t + f^{-1}J(\theta, \psi) - \beta L_\rho^2 \psi_x - \beta f^{-2}\theta_x\psi = g' w_e - 2g'D - 2g'S \tag{13}$$

where the Jacobian $J(A, B)$ is defined as

$$J(A, B) = A_x B_y - A_y B_x,$$

and L_ρ is the local deformation radius based on H_0:

$$L_\rho^2 = g' H_0 / f^2.$$

Equations (11) [or (12)] and (13) describe the time dependent baroclinic evolution of a two-layer ocean at basin scales and are remarkably similar to the two layer quasi-geostrophic equations. It is worth pointing out however that the phenomena described by the present model are in many ways richer than quasi-geostrophic phenomena. Layer thickness variations can be O(1) and the analysis is not restricted to the beta-plane. In addition, the time dependency of the baroclinic mode has been retained. The costs of including these effects are the introduction of some nonconstant coefficients and one nonlinear term in the prognostic equation. It thus appears that the numerical solution of these equations is not substantially more difficult than the numerical solution of the quasi-geostrophic equations. Work is currently under way on this topic.

Note that the lower layer in this model is ventilated by cross-isopycnal exchange [the S term in Eq. (13)]. This affects the potential vorticity dynamics of the lower layer by adding mass to it, in much the same way as Ekman pumping affects the potential vorticity dynamics of the upper layer. As discussed earlier, the magnitude of the potential vorticity forcing caused by S is proportional to the surface heat exchange. This is a different ventilation mechanism than that studied by Luyten et al., who assumed that the role of the buoyant forcing was to fix the outcropping latitudes of the lower layer isopycnals. The potential vorticity forcing in the lower layers of their model was provided solely by Ekman pumping.

b. *Quasi-geostrophic limit*

The numerical solutions of the complete model are currently under study. In the remainder of this paper, Eqs. (11), (12) and (13) will be examined in the parameter range corresponding to the steady state quasi-geostrophic limit at planetary scales (Pedlosky, 1979). As a result of adopting this scaling, the possibility of surfacing isopycnals will be lost. Ventilation of the lower layer will still be possible because of the cross-isopycnal exchange term, S. Some comparisons between these solutions and data will suggest that the model applies to the real ocean, and that the balances implied by the model are not overly dependent on the scaling. This assertion is also being tested numerically.

To obtain the steady, quasi-geostrophic equations, time derivatives are suppressed and the variables are scaled according to

$$\left.\begin{aligned} \psi &= f_0 U L \psi_* \\ \theta &= f_0 U L \theta_* \\ (x, y) &= L(x_*, y_*) \\ D &= D_0 D_* \\ S &= S_0 S_* \end{aligned}\right\} \quad (14)$$

where L is a basin scale length, $f_0 = 2\Omega \sin(\lambda_0)$ a reference Coriolis parameter, Ω the rotation rate of the earth, U a velocity scale, and the asterisks denote dimensionless variables. The nondimensional equations are (dropping the asterisks):

$$\beta\theta_x/\beta_0 + [\epsilon L^2/(2L_\rho^2)][\beta/\beta_0](\psi^2)_x = (f/f_0)^2 w_e \quad (15)$$

$$J(\theta, \psi) - \beta f_0/(f\beta_0)[\gamma\psi_x + \tilde{\beta}\psi\theta_x] = \beta f_0 \gamma/(f\beta_0)[\theta_x + \epsilon L^2/(2L_\rho^2)(\psi^2)_x] - \tilde{\beta} K D - \tilde{\beta}\alpha S \quad (16)$$

where

$$\left.\begin{aligned} \beta_0 &= 2\Omega \cos(\lambda_0)/a, \\ \tilde{\beta} &= \beta_0 L/f_0, \\ \epsilon &= U/f_0 L, \\ \gamma &= \beta L_\rho^2/U, \\ \alpha &= 2S_0 f/[\tilde{\beta}(f_0 U)^2], \\ K &= 2D_0 f/[\tilde{\beta}(f_0 U)^2] \end{aligned}\right\}.$$

Equation (2) has been used to scale the Ekman pumping, w_e. The nondimensional parameters $\epsilon = U/f_0 L$ (the Rossby number), $\tilde{\beta} = \beta_0 L/f_0$, α, and K arise from the preceding analysis and measure respectively, the strength of the mean flow relative vorticity compared to planetary vorticity, the variation of the Coriolis parameter over the gyre, the strength of the buoyancy forcing and the strength of eddy mixing. The parameter ordering for the quasi-geostrophic limit is

$$\epsilon \ll \epsilon L^2/L_\rho^2 \sim \tilde{\beta} \ll \gamma \sim \mathrm{O}(1).$$

The constraint on $\epsilon L^2/L_\rho^2$ restricts the layer thickness variations to small ones. Diabatic forcing and eddy diffusion are assumed to be weak; nondimensionally this is expressed by

$$K \sim \alpha \sim \mathrm{O}(1).$$

3. The quasi-geostrophic solution

The solution of Eqs. (15) and (16) is obtained by formally expanding the dependent variables θ and ψ in powers of $\tilde{\beta}$. The lowest order equations are

$$\theta_{0x} = w_e \quad (17)$$

$$J(\theta_0 + \gamma y, \gamma y - \psi_0) = 0. \quad (18)$$

Equation (17) may be integrated to yield

$$\theta_0 = \int_{x_e}^{x} w_e(x')dx',$$

and the solution to Eq. (18) is

$$\gamma y - \psi_0 = G(\theta_0 + \gamma y) = G(\chi) \tag{19}$$

where the function G is as yet undetermined. Note:

$$\psi_0 = p_2^0 - p_1^0$$

where p_2^0 and p_1^0 are the lowest order quantities in the perturbation expansion of the layer pressures; thus, the quantity:

$$\gamma y - \psi_0 = \gamma y - (p_2^0 - p_1^0) = q_0$$

is the lowest order contribution to the quasi-geostrophic lower layer potential vorticity. The other quantity in Eq. (19), $\chi = \theta_0 + \gamma y$, has been identified by Rhines and Young (1982b) as the geostrophic contours of the basin. Geostrophic contours are the lines of intersection of constant density and constant potential vorticity surfaces, and are therefore fluid trajectories. Equation (18) thus expresses the conservation of potential vorticity by fluid parcels.

The geostrophic contours can be computed given the wind forcing by solving Eq. (17). It is useful to consider the Sverdrup transport driven by the Ekman pumping:

$$\left.\begin{aligned} w_e &= -x, \quad x^2 + y^2 < 1 \\ w_e &= 0, \quad x^2 + y^2 > 1 \end{aligned}\right\}.$$

This forcing is known as "tilted disk" Ekman pumping, and has been used in the past to study the circulation structure in 'mid-ocean gyres' (Rhines and Young, 1982b). The net potential vorticity added by tilted disk pumping along a latitude line vanishes, which allows the barotropic Sverdrup transport lines to close in the oceanic interior without a western boundary layer. Using the above in Eq. (17), the geostrophic contours are

$$\left.\begin{aligned} \chi = \{1 - [x^2 + (y - \gamma)^2]\}/2 + \gamma^2/2, \quad x^2 + y^2 > 1 \\ \chi = \gamma y, \quad x^2 + y^2 < 1 \end{aligned}\right\}$$

and can close inside the basin depending on the parameter γ. In the spirit of Rhines and Young (1982a), I will assume the geostrophic contours close and form regions isolated from the eastern boundary (see Fig. 3a).

a. The lowest order solution in the interior

The lower layer is thus divided into the region of closed geostrophic contours and the "exterior." Solving for the lowest order solution requires knowing the structure function G in both regions. In the exterior, the fluid is directly connected via geostrophic contours to the eastern boundary, where the boundary conditions are

$$P_1^0 = P_2^0 = 0.$$

Thus on the eastern boundary, Eq. (19) may be written as

$$G(\gamma y) = \gamma y.$$

This determines the exterior form of G, as introducing the dummy variable Z:

$$G(Z) = Z.$$

The potential vorticity away from the eastern boundary is thus

$$\gamma y - \psi_0 = \gamma y + \theta_0$$

which implies

$$P_2^0 = 0.$$

The solution in the exterior region is consistent with vanishing lower layer flow, which, as is shown by the preceding analysis, is forced by the eastern no-flux condition.

Thus θ_0 in the exterior region is

$$\theta_0 = P_1^0$$

which determines P_1^0 through Eq. (17). Note also that outside of the regions of direct tilted disk forcing:

$$\theta_0 = 0.$$

This completes the lowest-order solution in the region outside of the closed geostrophic contours.

b. The dynamics inside the closed geostrophic contours

The mechanisms responsible for determining G inside the closed geostrophic contours should involve eddy mixing and forcing, both of which appear in the equations at the next order in $\tilde{\beta}$. The baroclinic equation at $O(\tilde{\beta})$ is

$$\begin{aligned} J(\theta_1, \psi_0) + J(\theta_0, \psi_1) - \gamma\psi_{1x} + \gamma \tan^2(\lambda_0)\psi_{0x} \\ + \gamma y\psi_{0x} - \psi_0\theta_{0x} - \gamma\theta_{1x} + \gamma \tan^2(\lambda_0)y\theta_{0x} \\ + \gamma\theta_{0x}y - (\psi_0^2/2)_x = -\alpha S - KD. \end{aligned} \tag{20}$$

If Eq. (20) is integrated over the area enclosed by a geostrophic contour, the left-hand side identically vanishes (see appendix B) leaving an integral balance between the diabatic sources of potential vorticity and eddy dissipation:

$$\alpha \iint_{A(\chi)} S dA + K \iint_{A(\chi)} D dA = 0 \tag{21}$$

where $A(\chi)$ denotes the area enclosed by a geostrophic contour. Further progress requires a closure theory to specify D. I will use the parameterization originally suggested by Rhines and Holland (1979) which equates eddy mixing and the lateral diffusion of potential vorticity:

$$D = \nabla^2 q. \tag{22}$$

This parameterization converts Eq. (21) into an equation for the potential vorticity structure inside the closed geostrophic contours:

$$\alpha \iint_{A(\chi)} SdA = -K \oint_{\partial A} \nabla q_0 \cdot \mathbf{n} dl = -K \left[\oint_{\partial A} \nabla \chi \cdot \mathbf{n} dl \right] G_\chi \tag{23}$$

where the line integral is along the bounding geostrophic contour, q_0 is the lowest order contribution to the potential vorticity and Eq. (19) has been used. The above equation can be further simplified by using the identity (Young, 1981):

$$\partial/\partial\chi \left[\iint_{A(\chi)} f(x, y) dA \right] = \oint_{\partial A} \{ f(x, y)/(\nabla\chi \cdot \mathbf{n}) \} dl,$$

in which case:

$$\alpha \oint [S/\nabla\chi \cdot \mathbf{n}] dl + \left\{ \left[K \oint \nabla\chi \cdot \mathbf{n} dl \right] G_\chi \right\}_\chi = 0. \tag{24}$$

The structure equation for the lower layer potential vorticity is a second-order, ordinary differential equation involving the Sverdrup transport and S. The integral coefficients in Eq. (24) can be determined using Eq. (17). The remainder of the problem can be closed by specifying the diabatic forcing. Note that the presence of the diabatic forcing modifies the structure of the solution importantly. If this model were adiabatic, as in Rhines and Young (1982a,b), potential vorticity homogenization would emerge from Eq. (23). The source term and the higher order equation in Eq. (24) will result in nontrivial structure in the interior of the gyre.

c. *The structure of the diabatic forcing*

Consider Fig. 2, taken from McDowell et al. (1982), which shows the annual variation in the outcropping latitudes of isopycnals in the North Atlantic. If 40°N is taken as the northern boundary of the subtropical gyre, some of the deeper isopycnals participating in the wind-driven gyre (e.g., the 26.3–26.5 sigma-theta layer) surface within the northern confines of the gyre during winter. Other, deeper layers (e.g., the 26.5–27.0 sigma-theta layer) do not outcrop even in late winter. Figure 2 points out two features of diabatic forcing which will be central to the following analysis. First, the tendency for the isopycnal outcrops to migrate south in the winter is consistent with a conversion of warm water to cold water, or equivalently a negative value for S. Second, the regions where this conversion will be most active are confined to the northern portion of the gyre. The simplest form for the forcing in the present model which retains these features is

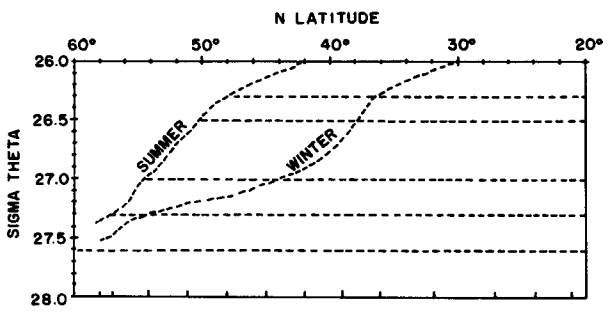

FIG. 2. Outcropping latitude variations. This figure originally appeared in McDowell et al. (1982, Fig. 15) and shows potential vorticity as a function of latitude and isopycnal. Note the 12° latitudinal variation in the surface outcrop of the shallower isopycnals. Taking 40°N as the northern limit of the subtropical gyre, the 26.3–26.5 surface is seen to be ventilated in late winter in the subtropical gyre. In contrast, the 26.5–27.0 surface appears not to be ventilated in the subtropical gyre.

$$\oint [S/\nabla\chi \cdot \mathbf{n}] dl = c_0 > 0, \quad \text{for} \quad \chi > \chi_c \tag{25a}$$

$$\oint [S/\nabla\chi \cdot \mathbf{n}] dl = 0, \quad \text{for} \quad \chi < \chi_c \tag{25b}$$

where c_0 is a positive constant and χ_c is the geostrophic contour which just grazes the southernmost limit of an otherwise limited area of diabatic forcing (see Fig. 3b). Choosing c_0 as a positive constant reflects the sense of the water mass production in the North Atlantic. Constraining nonzero values for S to occur in certain regions of the gyre models the northern confinement of ventilation. Note, the area of closed geostrophic contours is thus divided into two regions, an "interior" or "unventilated" region where $S = 0$, and a ventilated region.

It is unlikely that buoyancy forcing in the real ocean is arranged so that the integral in Eq. (25) is constant, but a constant is used here to simplify the problem as much as possible. I will argue shortly that the important features of the solution do not depend on this assumption.

d. *The solution inside the closed geostrophic contours*

In the interior where the diabatic forcing S vanishes, Eq. (24) simplifies to:

$$\left[K \oint (\nabla\chi \cdot \mathbf{n}) dl \right] \partial/\partial\chi G = \text{constant}. \tag{26}$$

The integral coefficient in Eq. (26) vanishes at the center of the gyre; thus, the right-hand side of Eq. (26) must be zero to avoid singularities. This implies:

$$G_\chi = 0,$$

or that the potential vorticity is homogeneous (at an as yet unknown value) in the interior of this partially ventilated layer.

Luyten et al. (1983) assumed uniform potential vorticity in the interior of their ventilated layers. The present analysis suggests this is justified. Note, however, that uniform potential vorticity depends upon dissipation.

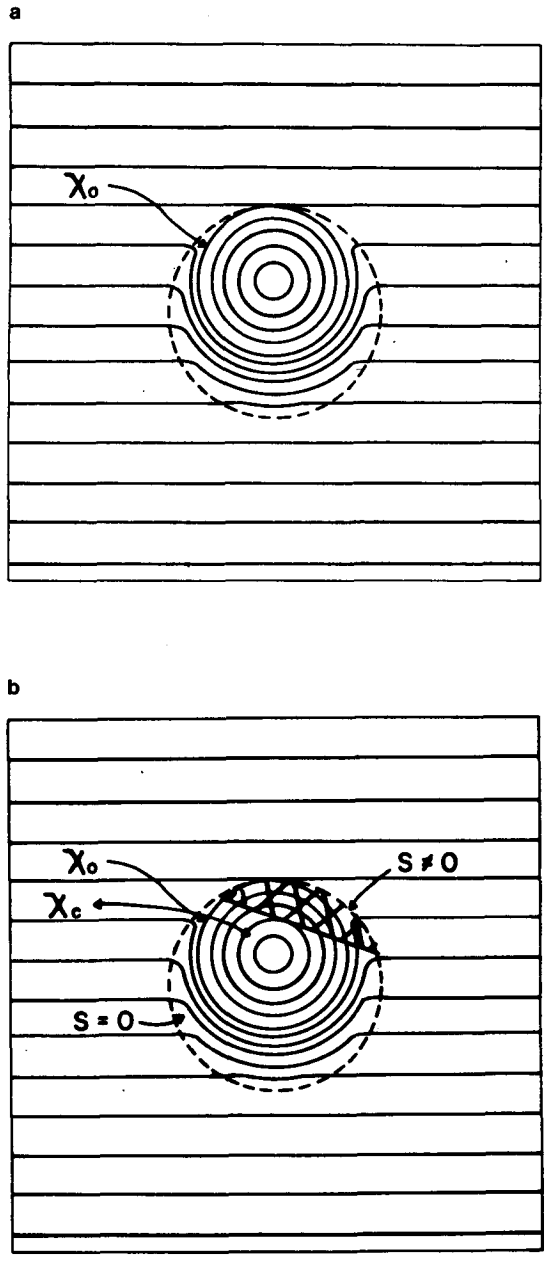

FIG. 3. (a) Geostrophic contours. If "tilted disk" Ekman pumping of sufficient strength is used, closed geostrophic contours like the above form in the lower layer. The area outside of χ_0, the largest closed geostrophic contour is called the exterior. (b) Same as in a, except the cross-hatched region indicates areas where the diabatic forcing is assumed to be nonzero. The closed geostrophic contours are divided into the interior, unventilated region and the ventilated region. The dividing contour between these regions, χ_c, is indicated.

In the ventilated region of the closed geostrophic contours, where Eq. (25a) applies, an integration of Eq. (24) yields

$$\left[\oint \nabla\chi \cdot \mathbf{n}dl\right] G_\chi = -c_0\alpha(\chi - \chi_c)/K \qquad (27)$$

where the constant has been used to match the zero potential vorticity flux at χ_c. The full solution for G in the ventilated region is

$$G(\chi) = [\alpha c_0/(4\pi K)](\chi - \chi_0) - [\alpha c_0/(8\pi K)] \times (1 + \gamma^2 - 2\chi_c) \ln\left(\frac{1 + \gamma^2 - 2\chi_0}{1 + \gamma^2 - 2\chi}\right) + q_f \quad (28)$$

where q_f is the potential vorticity on χ_0, the outermost closed geostrophic contour. Equation (28) can then be used to compute the value of the potential vorticity on χ_c. This in turn can be matched to the uniform potential vorticity in the unventilated part of the gyre interior to complete the solution. A graph of this solution is given in Fig. 4 for $\alpha c_0/(8\pi K) = 1$ and $\chi_c/\chi_0 = 0.25$. These parameter settings correspond to a gyre which is weakly ventilated in its northern quarter. An important aspect of the potential vorticity structure in Fig. 4 is that the region of uniform potential vorticity is a local minimum.

e. Frictional western boundary layer closures

Since S is of one sign (negative), net negative potential vorticity enters the lower layer within the closed geostrophic contours. This potential vorticity must be extracted from the gyre if the flow is to be steady. The only place where the extraction can occur is at the boundaries, and in keeping with homogeneous circulation theory, I will assume the western boundary dominates this process.

Note that the lowest order solution is consistent without boundary layers. The geostrophic contours

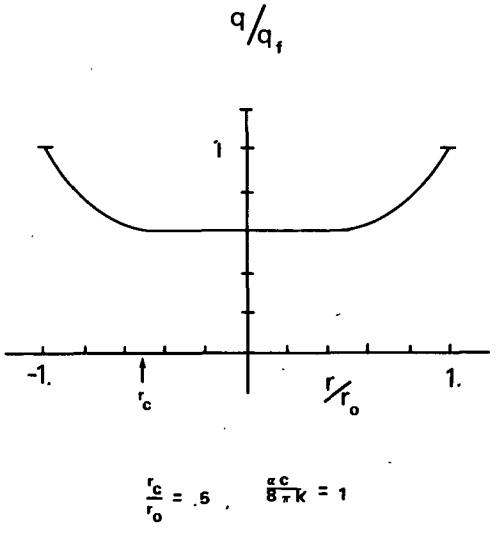

FIG. 4. Potential vorticity structure. The solution is divided into two regions: a homogenized potential vorticity region at gyre center, and a bowl-shaped region located towards the gyre edge. The two join smoothly. The bowl-shaped region is directly ventilated. The uniform potential vorticity is a local minimum, a result which depends only on down-gradient eddy mixing and a negative potential vorticity flux to the lower layer.

close away from the boundaries, and the exterior lower layer pressure solution, $P_2^0 = 0$, meets the required boundary conditions. The tilted-disk Ekman pumping is also confined to the basin interior, and the upper layer, lowest order pressure solution away from the directly forced region, $P_1^0 = 0$, also meets the required boundary conditions. The inconsistency in the solution is at $O(\tilde{\beta})$ and appears when Eq. (20) is integrated over the entire basin. It is not difficult to demonstrate that this integral reduces to

$$-\alpha \int\int_{\text{basin}} SdA = K \int\int_{\text{basin}} DdA = K \oint_{\partial \text{ basin}} \nabla q \cdot \mathbf{n} dl$$

where Eq. (22) has been used. If q is substituted for using the lowest order potential vorticity, the right hand side of the above vanishes, which is inconsistent with the imposed forcing. What is being neglected at $O(\tilde{\beta})$ in the baroclinic equation are the highest order terms, thus suggesting the need for a boundary layer involving the $O(\tilde{\beta})$ quantities.

Using Eq. (22), D can be written as

$$D = \nabla^2[\gamma y + (L_\rho^2/L^2)\nabla^2(P_2^0 + \tilde{\beta}P_2^1) + P_1^0 - P_2^0 + \tilde{\beta}(P_1^1 - P_2^1) + O(\tilde{\beta})^2]$$

where P_i^n denotes the nth member in the perturbation sequence for P_i.

Using the lowest order pressure solutions near the boundary yields:

$$D = \tilde{\beta}(L_\rho^2/L^2)\nabla^4 P_2^1 + \tilde{\beta}\nabla^2(P_1^1 - P_2^1) + O(\tilde{\beta}^2)$$

and Eq. (20) near the boundary becomes

$$2\gamma(P_2^1)_x = KD = K\tilde{\beta}(L_\rho^2/L^2)\nabla^4 P_2^1 + K\tilde{\beta}\nabla^2(P_1^1 - P_2^1).$$

Introducing the rescaled boundary layer coordinate $X = \delta^{-1}x$, the above can be written as:

$$2\gamma P_{2X}^1 = K\tilde{\beta}(L_\rho^2/L^2)\delta^{-3}P_{2XXXX}^1 + \delta^{-1}K\tilde{\beta}(P_1^1 - P_2^1)_{XX}.$$

The only consistent balance occurs if

$$\delta = [K\tilde{\beta}L_\rho^2/L^2]^{1/3}.$$

The governing equation in the boundary layer is thus the same as that for a Munk boundary layer:

$$2\gamma P_{2X}^1 = P_{2XXXX}^1$$

whose solution is

$$P_2^1(x, y) = P_{2I}^1(0, y) * \left\langle 1 - \exp\left[-(2\gamma)^{1/3}\delta^{-1}\frac{x}{2}\right] \times \left\{\cos\left[\frac{\sqrt{3}}{2}(2\gamma)^{1/3}\delta^{-1}x\right] + \frac{\sqrt{3}}{3}\sin\left[\frac{\sqrt{3}}{2}(2\gamma)^{1/3}\delta^{-1}x\right]\right\}\right\rangle$$

where P_{2I}^1 is the interior $O(\tilde{\beta})$ pressure. The boundary layer thickness is:

$$L\delta = [KL_\rho^2 L^2\beta/f_0]^{1/3}.$$

Using typical parameter values:

$$L\delta \approx 200 \text{ km}.$$

The magnitude of the northward flow in the boundary layer is

$$v_2(0, y) = \tilde{\beta}v_2^1 = O[\tilde{\beta}^2 L^2/(KL_\rho^2)]^{1/3}$$

and the north–south length scale of the boundary layer is determined by the vorticity balance:

$$\alpha \int\int SdA = -K\tilde{\beta}L_\rho^2/L^2 \int_{\substack{\text{western} \\ \text{boundary}}} P_{2XXX}^1 dy,$$

or

$$L_y = O(1).$$

If $\epsilon = O(\tilde{\beta}^2)$,

$$\left.\begin{aligned} v_2(0, y) &= O(\tilde{\beta})^{1/3} < 1 \\ \delta &= O(\tilde{\beta})^{2/3} < 1 \end{aligned}\right\},$$

indicating that the boundary layer is weak and rather broad.

4. Generalization and interpretation of results

The integral balance in Eq. (21), which determines the potential vorticity structure in the model, is between buoyancy forcing and eddy diffusion. It states that the net diffusive loss of potential vorticity on every streamline cancels the addition of potential vorticity on that streamline due to buoyant forcing. Warm water is converted to cold water by atmospheric exchange in the northern half of the North Atlantic subtropical gyre. The deeper isopycnals are thus receiving mass from the shallower isopycnals, which translates into a source of negative potential vorticity for the deeper layers. The integral balance in Eq. (23) requires the eddies to diffusively add positive potential vorticity to each streamline. The only source of positive potential vorticity in the lower layer is the ocean boundary, so all the positive q needed to balance the negative diabatically injected q comes from outside the closed lower layer geostrophic contours. This is evident if Eq. (23) is evaluated at χ_0. If the eddies move potential vorticity down the mean potential vorticity gradient, the overall forcing-dissipation balance requires the mean potential vorticity inside the closed contours to be lower in value than the exterior potential vorticity. This is why the q structure decreases toward gyre center and why the homogenized pool is a minimum.

Note, the balance between buoyancy forcing and eddy diffusion makes no explicit reference to quasi-geostrophy. The structure of the solution requires that the eddies effect a potential vorticity flux with a component pointing down the mean gradient and that

warm waters are being converted to cold waters. It is therefore likely that the characteristics of the present solution will appear in systems which are not quasi-geostrophic.

5. Comparison with data

McDowell et al. (1982) have analyzed the GEOSECS data from the North Atlantic in terms of potential vorticity. Two of their figures (Figs. 17 and 18) are included in Fig. 5 for completeness. These are diagrams of potential vorticity as a function of latitude on the 26.3–26.5 and 26.5–27.0 sigma-theta surfaces, and are in surprisingly good agreement with the predictions of the present theory.

Figure 5a illustrates the potential vorticity in the 26.3–26.5 layer, an isopycnal which is ventilated for a fraction of the year by wintertime convection (see Fig. 2). The net potential vorticity input into this layer is weak, making it ideal for comparison with the present theory. Note the characteristic bowl shape of the potential vorticity with the minimum occurring at the gyre center. There is even a hint of a homogenized region between 25° and 35°N. The present theory suggests this structure is the result of lateral potential vorticity mixing and diabatic potential vorticity forcing.

It is interesting to compare the potential vorticity structure in the 26.3–26.5 layer with that in the deeper 26.5–27.0 layer, shown in Fig. 5b. The 26.5–27.0 layer is not ventilated at any time during the year (see Fig. 2). This layer is characterized by homogeneous potential vorticity, a result predicted by Eq. (23) if $S = 0$, or equivalently if the layer is adiabatic. The difference in the potential vorticity structure on the neighboring 26.3–26.5 and 26.5–27.0 layers is striking. It is encouraging that the present model explains both.

Several other characteristics of the model are seen in the data. In Fig. 5 of McDowell et al. (1982), a plan view of the potential vorticity on the 26.3–26.5 surface is presented along with an estimate of the late winter outcrop latitudes. In agreement with the model, the strongest potential vorticity gradients occur in regions which are directly ventilated. Other areas which are not directly ventilated have weaker q structure. This to an extent also describes the 26.0–26.3 surface (Fig. 4 in McDowell et al.), which is somewhat more strongly ventilated than the deeper 26.3–26.5 layer, suggesting that the present theory applies beyond the parameter settings of the analytical solutions.

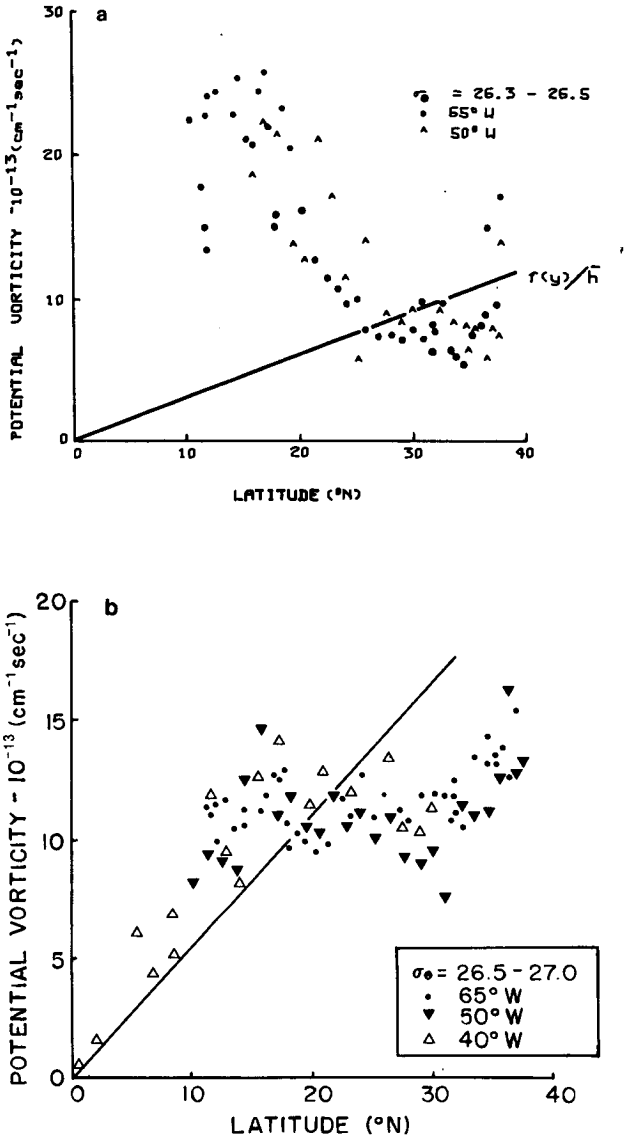

FIG. 5. Potential vorticity on potential density surfaces in the North Atlantic. These figures appeared originally in McDowell et al. (1982, Figs. 17 and 18) and show the potential vorticity structure on the σ_θ = 26.3–26.5 surface and the σ_θ = 26.5–27.0 surface. The shallower σ_θ = 26.3–26.5 surface is weakly ventilated, and obtains the bowl shape predicted by theory. There is also a hint of uniform potential vorticity between 25° and 35°N. This area corresponds to 18°C water. The deeper layer (σ_θ = 26.5–27.0) is not ventilated, and exhibits no such bowl-like structure.

6. Discussion

A layer model of the general circulation employing linear potential vorticity dynamics in each layer has been used to study the effects of diabatic forcing. This model admits analytical solutions in the quasi-geostrophic, weakly forced limit, which are characterized by a balance between diabatic input and eddy mixing. These solutions are a generalization of those found by Rhines and Young (1982b), where ventilation was ignored, and by Luyten et al. (1983) who ignored dissipative effects.

Unlike the Luyten et al. model, the present model resolves the potential vorticity structure in regions of ventilated layers not directly connected to outcrops. Luyten et al. assumed that these regions were homogeneous in potential vorticity. The present model supports this assumption, but demonstrates that uniform

potential vorticity is a result of mixing. Dissipative effects are also not confined to unventilated areas; rather, their influence is global and alters the q structure on streamlines which are directly ventilated. In this sense, the present theory differs substantially from Luyten et al. or Rhines and Young. Many features of the potential vorticity in of the North Atlantic can be explained by the present theory, suggesting that the theory has some analogs in the real ocean.

The wind stress employed here simplifies model western boundary layer structure by adding no net potential vorticity to the ocean. Although analytically convenient, this is obviously a weak point of the model. More realistic wind stress patterns can invalidate some of the assumptions leading to the integral balance in Eq. (21). This was demonstrated for a simple general circulation model by Ierley and Young (1983). In their model, the lower layer failed to homogenize in potential vorticity due to the presence of a strongly dissipative lower layer western boundary current. If, however, dissipation occurs preferentially in the surface layers of the ocean (possibly through some mechanism involving relative vorticity), as postulated by Young and Rhines, friction may still be regarded as weak everywhere in the lower layer and the analysis proceeds as in the present theory. Tilted disk Ekman pumping is a convenient way of modeling weak potential vorticity dissipation in the lower layer while retaining a tractible model. It is nonetheless true that the details of the homogenization process are not yet well understood. It has also been necessary to include a weak frictional western boundary layer to close the global potential vorticity budget. The characteristics of this boundary layer have been described.

In some sense, this model takes some tentative steps toward a fully ventilated general circulation model with an explicit western boundary layer. It is worth stressing that most of the lower-layer streamlines do not require strong, local western boundary layer dissipation, even though the lower layer receives net vorticity. Instead, eddy mixing acts everywhere on the streamlines and moves the injected potential vorticity towards the gyre edges, so that it is only the outer few streamlines which must pass through a frictional boundary layer. Thus the present model is only weakly dependent on boundary layers, which lends weight to those models in which boundary layers are ignored (Luyten et al., 1983; Pedlosky and Young, 1983). One wonders if similar processes reduce dissipative effects on streamlines in models with stronger vorticity input.

Mode waters. An important application of this work is to the maintenance and stability of mode waters in subtropical gyres. The present theory predicts that weakly ventilated layers will have a central pool of uniform potential vorticity which is at a local minimum. This pool corresponds to mode water in the usual sense of either thick layers (small f/h) or weak vertical density gradients (small $f\rho_z$) and exists in this model because of the interaction of lateral eddy mixing and weak ventilation. Furthermore, this result depends only on S being negative and eddy mixing being down-gradient in sense. It is interesting that the σ_θ = 26.3–26.5 isopycnal surface, which is apparently well suited for comparison with the present theory, lies at the heart of the 18°C water in the North Atlantic (Worthington, 1959, Talley and Raymer, 1982; Jenkins, 1982).

It has been noted that the properties of 18°C water are stable in spite of considerable meteorological variability at the source regions. This has been discussed theoretically by Warren (1972), and led Talley and Raymer (1982) and Jenkins (1982) to conclude that some global storage mechanism must be in operation which buffers 18°C water against climatic variability. The present solutions reflect precisely this behavior. The diffusive balance expressed in Eq. (21) makes the potential vorticity structure in Fig. 4 largely insensitive to seasonal variability in buoyancy forcing. Local disturbances in the potential vorticity structure, as would be produced by an anomalously cold winter, will be considerably reduced in effect by mixing. In addition, the gyre has a lot of inertia. Although time dependent calculations have yet to be done, it is likely that the gyre adjusts on cross-gyre diffusion time scales (Dewar et al., 1984), which are about ten years:

$$\frac{L^2}{4K} = \frac{(10^8\ \text{cm})^2}{4 \times 10^7\ \text{cm}^2\ \text{s}^{-1}} = 10\ \text{years}.$$

In order to produce variability in the properties of 18°C water, anomalies in the source regions must persist for roughly a decade. Because of the gyre inertia, variations in the properties of the mode water will also lag the forcing by roughly a decade. This agrees with the time scale of temperature and salinity variability within the 18°C water noted by Jenkins (1982).

Acknowledgments. This work has benefited from conversations with Drs. William R. Young, Peter B. Rhines and John M. Bane. It is a pleasure to recognize their interest and scientific input. Several figures in this paper appeared originally in a paper by S. McDowell, P. Rhines and T. Keffer, and are reproduced here by their kind permission. This paper was typed by Shirley Kilpatrick and Pat Klein. The figures were prepared by Cyndi Louden and Jane M. McManus. My research is sponsored by NSF Grant OCE-8415475 to the University of North Carolina.

APPENDIX A

Heat Balance in a Two-Layer Fluid

The heat equation for a continuously stratified Boussinesq fluid is:

$$T_t + uT_x + vT_y + wT_z = -\nabla \cdot F \qquad \text{(A1)}$$

where T is temperature, u and v are horizontal velocities, w is vertical velocity, subscripts denote differen-

tiation, $F = (F^{(x)}, F^{(y)}, F^{(z)})$ is an internal heat flux vector and, for convenience, a Cartesian coordinate system has been adopted. The heat equation for a two layer fluid can be formally obtained by substituting for T with:

$$T = T_2 + \Delta T\{\text{erf}[(z + h)/\delta] - \text{erf}[(-H + h)/\delta]\} \quad \text{(A2)}$$

where

$$\left.\begin{aligned}\text{erf}[(z + h)/\delta] &= (\sqrt{2\pi})^{-1} \int_{-\infty}^{(z+h)/\delta} e^{-Z^2/2} dZ \\ \text{erf}[(-H + h)/\delta] &= (\sqrt{2\pi})^{-1} \int_{-\infty}^{(-H+h)/\delta} e^{-Z^2/2} dZ\end{aligned}\right\};$$

T_2 is the bottom temperature, ΔT the maximum possible temperature change in the water column, h a function of x, y, and t, and δ a parameter controlling the vertical thickness over which the temperature change occurs; ΔT is a constant. Note that as δ becomes small, T tends to a two-layer temperature distribution with lower layer temperature T_2 and upper layer temperature $T_1 = T_2 + \Delta T$. The transition between these two layers occurs discontinuously at the interface, $z = -h$.

The velocities u, v and w are assumed to be of the form:

$$u = u_2(x, y, z, t) + \Delta u(x, y, z, t) \times \{\text{erf}[(z + h)/\delta] - \text{erf}[(-H + h)/\delta]\} \quad \text{(A3)}$$

$$v = v_2(x, y, z, t) + \Delta v(x, y, z, t) \times \{\text{erf}[(z + h)/\delta] - \text{erf}[(-H + h)/\delta]\} \quad \text{(A4)}$$

$$w = w_2(x, y, z, t) + \Delta w(x, y, z, t) \times \{\text{erf}[(z + h)/\delta] - \text{erf}[(-H + h)/\delta]\} \quad \text{(A5)}$$

where $u_2(x, y, -H, t)$, $v_2(x, y, -H, t)$ and $w_2(x, y, -H, t)$ are the fluid velocities at the bottom and Δu, Δv and Δw are related to the velocity changes caused by the temperature structure. The quantities u_2, v_2, w_2, Δu, Δv and Δw are in general functions of x, y, z and t, but are assumed to be independent of the parameter δ. Note that as δ becomes small, u, v and w tend toward velocity distributions with a discontinuity at the interface $z = -h$.

The form of the derivatives of T can be demonstrated by considering T_t:

$$T_t = \Delta T h_t (e^{-(z+h)^2/2\delta^2} - e^{-(-H+h)^2/2\delta^2})/(\sqrt{2\pi}\delta)$$

thus Eq. (A1) becomes

$$\Delta T[h_t + uh_x + vh_y + w] \frac{e^{-(z+h)^2/2\delta^2}}{\sqrt{2\pi}\delta} - \Delta T(h_t + uh_x + vh_y) \frac{e^{-(-H+h)^2/2\delta^2}}{\sqrt{2\pi}\delta} = -\nabla \cdot \mathbf{F}. \quad \text{(A6)}$$

Equation (A6) demonstrates that as δ becomes small:

$$\nabla \cdot \mathbf{F} = 0 \quad \text{for} \quad z + h \neq 0$$

or that in a two-layer fluid, the internal heat fluxes must be nondivergent away from the interface. If it is further assumed that lateral heat fluxes can be ignored, Eq. (A7) becomes

$$F_z^{(z)} = 0 \quad \text{(A7)}$$

where $F^{(z)}$ is the vertical heat flux. Equation (A7) demonstrates that in a two-layer fluid:

$$F^{(z)}(z = -h) = F^{(z)}(z = 0) = F_s$$

where F_s is the heat flux to the atmosphere from the ocean.

Integrating Eq. (A6) over the interface from $-h - \nu$ to $-h + \nu$ yields

$$\Delta T h_t[\text{erf}(\nu/\delta) - \text{erf}(-\nu/\delta)] + \Delta T h_x \int_{-h-\nu}^{-h+\nu} \frac{ue^{-(z+h)^2/2\delta^2}}{\sqrt{2\pi}\delta} dz + \Delta T h_y \times \int_{-h-\nu}^{-h+\nu} \frac{e^{-(z+h)^2/2\delta^2}}{\sqrt{2\pi}\delta} dz + \Delta T \int_{-h-\nu}^{-h+\nu} \frac{we^{-(z+h)^2/2\delta^2}}{\sqrt{2\pi}\delta} \times dz + O(e^{-(-H+h)^2/2\delta^2}) = -F_s \quad \text{(A8)}$$

where it has been assumed that the internal heat fluxes under the interface vanish and the exponentials proportional to $-(H + h)/\delta$ have been ignored in anticipation of letting δ go to zero. The first term tends to $\Delta T h_t$ as δ becomes small. Substituting for u in the next integral yields

$$\int_{-h-\nu}^{-h+\nu} \langle u_2 + \Delta u\{\text{erf}[(z + h)/\delta] - \text{erf}[(-H + h)/\delta]\}\rangle \times \frac{e^{-(z+h)^2/2\delta^2}}{\sqrt{2\pi}\delta} dz = \int_{-h-\nu}^{-h+\nu} \frac{u_2 e^{-(z+h)^2/2\delta^2}}{\sqrt{2\pi}\delta} dz + \int_{-h-\nu}^{-h+\nu} \Delta u \,\text{erf}[(z + h)/\delta] \frac{e^{-(z+h)^2/2\delta^2}}{\sqrt{2\pi}\delta} dz + O(e^{-[(-H+h)^2/2\delta^2]}). \quad \text{(A9)}$$

In the limit of small δ:

$$\lim_{\delta \to 0} \int_{-h-\nu}^{-h+\nu} u_2(x, y, z, t) \frac{e^{-(z+h)^2/2\delta^2}}{\sqrt{2\pi}\delta} \times dz \to u_2(x, y, -h, t).$$

The second integral in Eq. (A9) can be rewritten as

$$\int_{-h-\nu}^{-h+\nu} \Delta u/2\{\text{erf}^2[(z + h)/\delta]\}_z dz = \Delta u(x, y, -h)/2 - 1/2 \int_{-h-\nu}^{-h+\nu} \text{erf}^2[(z + h)/\delta](\Delta u)_z dz$$

in the limit of small δ. The second integral on the right hand side is $O(\nu)$ as Δu is independent of δ, and therefore bounded in the limit of small δ. Thus Eq. (A8) in the limit of small δ tends to

$$\Delta T h_t + \Delta T h_x(u_2 + \Delta u/2) + \Delta T h_y(v_2 + \Delta v/2) + \Delta T(w_2 + \Delta w/2) = -F_s + O(\nu). \quad \text{(A10)}$$

The continuity equation for a Boussinesq fluid is

$$u_x + v_y + w_z = 0, \quad \text{(A11)}$$

which when integrated over the interface at $z = -h$ yields

$$[u(-h + \nu) - u(-h - \nu)]h_x + [v(-h + \nu) - v(-h - \nu)]h_y + w(-h + \nu) - w(-h - \nu) = 0.$$

Substituting with Eqs. (A3)–(A5) yields

$$\Delta w(x, y, -h) + \Delta u(x, y, -h)h_x + \Delta v(x, y, -h)h_y = 0(\nu)$$

in the limit of small ν. Defining

$$\left.\begin{aligned} u_1 &= u_2(x, y, -h) + \Delta u(x, y, -h) \\ v_1 &= v_2(x, y, -h) + \Delta v(x, y, -h) \\ w_1 &= w_2(x, y, -h) + \Delta w(x, y, -h) \end{aligned}\right\},$$

Eq. (A10) becomes

$$\Delta T(h_t + u_1 h_x + v_1 h_y + w_1) = -F_s. \quad \text{(A12)}$$

Dividing by ΔT and Reynolds averaging yields

$$\bar{w}_1(x, y, -h) = -\bar{h}_t - \bar{u}_1\bar{h}_x - \bar{v}_1\bar{h}_y - \overline{u_1'h_x'} - \overline{v_1'h_y'} - \bar{F}_s/\Delta T = -\bar{h}_t - \bar{u}_1\bar{h}_x - \bar{v}_1\bar{h}_y + D + S \quad \text{(A13)}$$

where D is the "thickness flux" associated with the eddies, S is the contribution to the interface movement due to surface heat fluxes, the overbars denote Reynolds averaged quantities and the primes denote fluctuating quantities. Except for the overbars and the use of Cartesian coordinates, Eq. (A13) is the same as Eq. 10 in the text.

APPENDIX B

Integral Balance in the Gyre

After a little algebra, the baroclinic evolution equation [Eq. (20)] can be written as

$$J(\theta_1, \psi_0 - \gamma y) + J(\theta_0 + \gamma y, \psi_1) + [\gamma \tan^2(\lambda_0) y\psi_0]_x + \gamma y\psi_{0x} + [\gamma \tan^2(\lambda_0) y\theta_0]_x + \gamma[\theta_0 y]_x + \frac{1}{2}(\psi_0^2)_x - \psi_0\theta_{0x} = -\alpha S - KD. \quad \text{(B1)}$$

Area integrals over closed geostrophic contours of the Jacobians vanish identically. For example, in the case of the first Jacobian:

$$\iint_{A(\chi)} J(\theta_1, \psi_0 - \gamma y)dA = \oint_{\partial A} \tilde{\mathbf{v}} \cdot \mathbf{n}\theta_1 dl$$

where

$$\tilde{\mathbf{v}} = [(\psi_0 - \gamma y)_y, -(\psi_0 - \gamma y)_x] = G_\chi(\chi_y, -\chi_x),$$

so that

$$\left.\begin{aligned} \tilde{\mathbf{v}} \cdot \mathbf{n} &= 0 \\ \iint_{A(\chi)} J(\theta_1, \psi_0 - \gamma y)dA &= 0 \end{aligned}\right\}.$$

A similar proof applies to the second Jacobian. The next four quantities in Eq. (B1) can each be written in the form $[p(y)N(\chi)]_x$, where p and N are functions only of y and χ respectively. Area integrals of these terms return:

$$\iint_{A(\chi)} [p(y)N(\chi)]_x dA = \oint_{\partial A} p(y)N(\chi)\mathbf{i} \cdot \mathbf{n}dl = N(\chi) \oint_{\partial A} p(y)dy = 0$$

using the fact that the line integral is along a contour of constant χ. The last quantity on the left hand side of Eq. (B1) when area integrated can be shown to vanish as follows:

$$\iint \psi_0\theta_{0x}dA = \iint \psi_0\chi_x dA = -\iint \chi q_{0x}dA = -\iint L(\chi)_\chi \chi_x dA = -\iint L(\chi)_\chi dA = 0$$

where $L(\chi)$ is defined by

$$L(\chi)_\chi = \chi q_0(\chi)_\chi.$$

Thus, Eq. (B1) reduces to

$$0 = \alpha \iint_{A(\chi)} SdA + K \iint_{A(\chi)} DdA,$$

which is Eq. (21).

REFERENCES

Dewar, W. K., P. B. Rhines and W. R. Young, 1984: The nonlinear spin-up of a stratified ocean. *Geophys. Astrophys. Fluid Dyn.*, **30**, 169–197.

Ierley, G., and W. Young, 1983: Can the western boundary layer affect the potential vorticity distribution in the Sverdrup interior of a wind gyre? *J. Phys. Oceanogr.*, **13**, 1753–1763.

Jenkins, W. J., 1982: On the climate of a subtropical ocean gyre: Decade time-scale variations in water mass renewal in the Sargasso Sea. *J. Mar. Res.*, **40**(Suppl), 265–290.

Keffer, T., 1985: The ventilation of the world's oceans: maps of the potential vorticity field. *J. Phys. Oceanogr.*, **15,** 509–523.

Leetma, A., P. P. Niiler and H. Stommel, 1977: Does the Sverdrup relation account for the mid-Atlantic circulation? *J. Mar. Res.*, **35,** 1–10.

Luyten, J., T. Pedlosky and H. Stommel, 1983: The ventilated thermocline. *J. Phys. Oceanogr.*, **13,** 292–309.

McDowell, S., P. B. Rhines and T. Keffer, 1982: North Atlantic potential vorticity and its relation to the general circulation. *J. Phys. Oceanogr.*, **12,** 1417–1436.

Pedlosky, J., 1979: *Geophysical Fluid Dynamics.* Springer, 624 pp.

——, and W. R. Young, 1983: Ventilation, potential-vorticity homogenization and the structure of the ocean circulation. *J. Phys. Oceanogr.*, **13,** 2020–2037.

Rhines, P. B., 1984: A discussion of the wind-driven circulation: the role of gyration. *J. Phys. Oceanogr.*, submitted.

——, and W. R. Holland, 1979: A theoretical discussion of eddy-driven mean flows. *Dyn. Atmos. Oceans,* **3,** 289–325.

——, and W. R. Young, 1982a: Homogenization of potential vorticity in planetary gyres. *J. Fluid Mech.*, **122,** 347–367.

——, and ——, 1982b: A theory of the wind-driven circulation, I. Mid-ocean gyres. *J. Mar. Res.*, **40**(Suppl.), 559–596.

Talley, L. D., and M. E. Raymer, 1982: Eighteen degree water variability. *J. Mar. Res.*, **40**(Suppl.), 757–775.

Warren, B., 1970: General circulation of the South Pacific. *Scientific Exploration of the South Pacific,* Natl. Acad. Sci., 33–49.

——, 1972: The insensitivity of subtropical mode water characteristics to meteorological fluctuations. *Deep–Sea Res.*, **19,** 1–20.

Worthington, L. V., 1959: The 18° water in the Sargasso Sea. *Deep–Sea Res.*, **5,** 297–305.

Young, W. R., 1981: The vertical structure of the wind-driven circulation. MIT-WHOI Ph.D. thesis, WHOI Tech. Rep. WHOI-81-89, unpublished manuscript.

——, and P. B. Rhines, 1982: A theory of the wind-driven circulation, II. Gyres with western boundary layers. *J. Mar. Res.*, **40,** 849–872.